

**Pressure-driven transport of confined DNA polymers in fluidic channels**

Derek Stein, Frank H. J. van der Heyden, Wiepke J. A. Koopmans, and Cees Dekker

*PNAS* 2006;103;15853-15858; originally published online Oct 17, 2006;  
doi:10.1073/pnas.0605900103**This information is current as of December 2006.**

<b>Online Information &amp; Services</b>	High-resolution figures, a citation map, links to PubMed and Google Scholar, etc., can be found at: <a href="http://www.pnas.org/cgi/content/full/103/43/15853">www.pnas.org/cgi/content/full/103/43/15853</a>
<b>References</b>	This article cites 18 articles, 7 of which you can access for free at: <a href="http://www.pnas.org/cgi/content/full/103/43/15853#BIBL">www.pnas.org/cgi/content/full/103/43/15853#BIBL</a>  This article has been cited by other articles: <a href="http://www.pnas.org/cgi/content/full/103/43/15853#otherarticles">www.pnas.org/cgi/content/full/103/43/15853#otherarticles</a>
<b>E-mail Alerts</b>	Receive free email alerts when new articles cite this article - sign up in the box at the top right corner of the article or <a href="#">click here</a> .
<b>Rights &amp; Permissions</b>	To reproduce this article in part (figures, tables) or in entirety, see: <a href="http://www.pnas.org/misc/rightperm.shtml">www.pnas.org/misc/rightperm.shtml</a>
<b>Reprints</b>	To order reprints, see: <a href="http://www.pnas.org/misc/reprints.shtml">www.pnas.org/misc/reprints.shtml</a>

Notes:

# Pressure-driven transport of confined DNA polymers in fluidic channels

Derek Stein, Frank H. J. van der Heyden, Wiepke J. A. Koopmans, and Cees Dekker<sup>†</sup>

Kavli Institute of Nanoscience, Delft University of Technology, Delft 2611 RL, The Netherlands

Communicated by Robert H. Austin, Princeton University, Princeton, NJ, July 17, 2006 (received for review January 20, 2006)

The pressure-driven transport of individual DNA molecules in 175-nm to 3.8- $\mu\text{m}$  high silica channels was studied by fluorescence microscopy. Two distinct transport regimes were observed. The pressure-driven mobility of DNA increased with molecular length in channels higher than a few times the molecular radius of gyration, whereas DNA mobility was practically independent of molecular length in thin channels. In addition, both the Taylor dispersion and the self-diffusion of DNA molecules decreased significantly in confined channels in accordance with scaling relationships. These transport properties, which reflect the statistical nature of DNA polymer coils, may be of interest in the development of “lab-on-a-chip” technologies.

nanofluidics

Transport of DNA and proteins within microfluidic and nanofluidic channels is of central importance to “lab-on-a-chip” bioanalysis technology. As the size of fluidic devices shrinks, a new regime is encountered where critical device dimensions approach the molecular scale. The properties of polymers like DNA often depart significantly from bulk behavior in such systems because statistical properties or finite molecular size effects can dominate there. DNA confinement effects have been exploited in novel diagnostic applications such as artificial gels (1), entropic trap arrays (2), and solid-state nanopores (3, 4). These advances underline the importance of exploring the fundamental behavior of flexible polymers in fluid flows and channels (5–10) that underlie current and future fluidic technologies.

Most transport in microfluidic and nanofluidic separation applications is currently driven by electrokinetic mechanisms that result in a uniform velocity profile and low dispersion (11, 12). An applied pressure gradient, in contrast, generates a parabolic fluid velocity profile that is maximal in the channel center and zero at the walls. Many important aspects of pressure-driven flows as a transport mechanism remain unexplored despite their ease of implementation and their ubiquity in conventional chemical analysis techniques such as high-pressure liquid chromatography. Our understanding of an object’s fundamental transport properties in parabolic flows, mobility and dispersion, is at present based mainly on models for rigid particles (13, 14) that explain several important effects such as the following: (i) hydrodynamic chromatography, the tendency of large particles to move faster than small particles because large particles are more strongly confined to the center of a channel, where the flow speeds are highest, and (ii) Taylor dispersion (15), the mechanism by which analyte molecules are hydrodynamically dispersed as they explore different velocity streamlines by diffusion, an effect that has discouraged the use of pressure-driven flows in microfluidic separation technology. The applicability of rigid-particle models as useful approximations to the transport of flexible polymers is dubious in the regime where the channel size is comparable with the characteristic molecular coil size, the radius of gyration ( $R_g$ ), yet remains untested there.

In this work, we present an investigation of the pressure-driven mobility and dispersion of individual DNA molecules in mi-

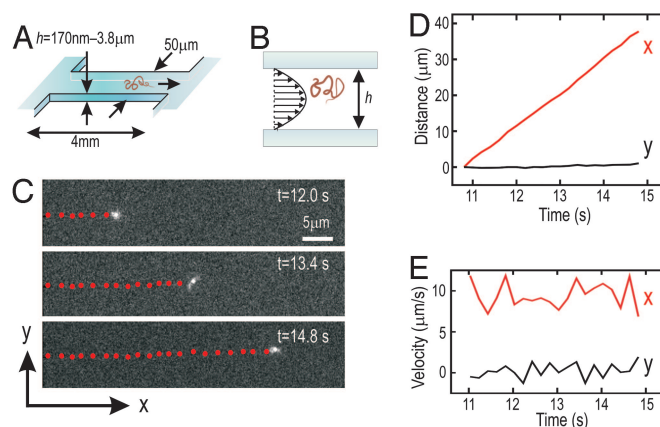


**Fig. 1.** Experimental observation of pressure-driven DNA transport in microfluidic and nanofluidic channels. (A and B) Schematic illustrations of a rectangular, 50- $\mu\text{m}$ -wide, 4-mm-long silica fluidic channel (A) and the channel cross-section over which an applied pressure gradient generates a parabolic fluid velocity profile (B). (C) Imaging a fluorescently labeled 48.5-kbp DNA molecule as it was transported through an  $h = 250$  nm channel by an applied pressure gradient of  $1.44 \times 10^5$  Pa/m. The red dots indicate the center-of-mass positions, recorded at a rate of 5 Hz. (D) The molecular trajectory along ( $x$  direction) and perpendicular to ( $y$  direction) the fluid flow, as a function of time. The linear increase in  $x$  position over time indicates a well defined average pressure-driven velocity. No net velocity is observed in the  $y$  direction. (E) The  $x$  and  $y$  components of the instantaneous molecular velocity as a function of time. The fluctuations along the flow are analyzed to study Taylor dispersion. The  $y$  direction fluctuations are independent of applied pressure and reflect thermal self-diffusion alone.

crofluidic and nanofluidic channels that reveals how this behavior is rooted in the statistical properties of polymer coils. DNA mobility exhibits both length-dependent and -independent regimes, while both the Taylor dispersion and the self-diffusion of DNA are observed to be strongly reduced in confined channels, in accordance with scaling relationships.

## Results and Discussion

Microfluidic and nanofluidic channels (illustrated in Fig. 1A and B) were filled with aqueous buffer containing fluorescently labeled DNA molecules that were imaged by epifluorescence video microscopy. The three types of linear DNA fragment studied had lengths,  $L$ , of 48.5 kbp (22  $\mu\text{m}$ ), 20.3 kbp (9.2  $\mu\text{m}$ ), and 8.8 kbp (4  $\mu\text{m}$ ). The corresponding equilibrium DNA coil sizes (16) ( $R_g = 0.73, 0.46,$  and  $0.29$   $\mu\text{m}$ , respectively) lie within the 175 nm to 3.8  $\mu\text{m}$  range of the channel height,  $h$ . DNA molecules were transported along the channel by means of an applied pressure gradient,  $p$ , that was controlled by adjusting the

Author contributions: D.S. and C.D. designed research; D.S. and W.J.A.K. performed research; F.H.J.v.d.H. contributed new reagents/analytic tools; D.S. and F.H.J.v.d.H. analyzed data; and D.S. wrote the paper.

The authors declare no conflict of interest.

<sup>†</sup>To whom correspondence should be addressed. E-mail: dekker@mb.tn.tudelft.nl.

© 2006 by The National Academy of Sciences of the USA







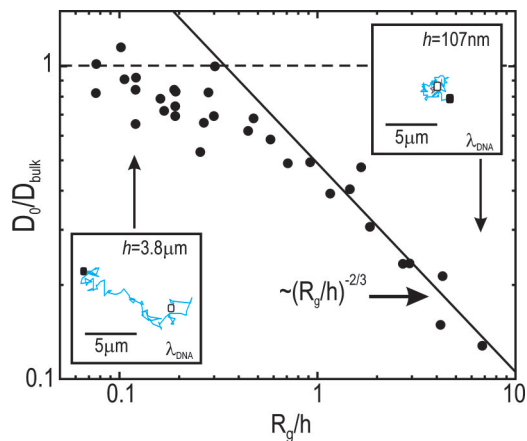


**Fig. 4.** Dependence of the normalized molecular self-diffusivity on the normalized channel height. The ratio  $D_0/D_{\text{bulk}}$  is plotted as a function of  $R_g/h$  for all molecular lengths. (Insets) The self-diffusion trajectories of  $\lambda$ -DNA molecules in  $h = 3.8 \mu\text{m}$  and  $h = 107 \text{ nm}$  channels, observed over a 20-s interval. The trajectories originate at the filled square and terminate at the open square.

Although DNA is an extended statistical object, the convective component of DNA dispersion in thin microfluidic and nanofluidic channels is consistent with a point-like solute description, i.e.,  $\alpha_T = 0.038 \times h^2/D_{\text{eff}}$ , where the effective DNA diffusion coefficient,  $D_{\text{eff}}$ , scales as  $D_{\text{eff}} \propto \sqrt{L}$ . From the fit to our data, we find  $D_{\text{eff}} \approx 9.9 \mu\text{m}^{3/2}\cdot\text{s}^{-1} \times \sqrt{L}$ . This result is in stark contrast to the bulk diffusion constant,  $D_{\text{bulk}}$ , which is known to obey  $D_{\text{bulk}} = 4.5 \mu\text{m}^{2+0.611}\cdot\text{s}^{-1} \times 1/L(\mu\text{m})^{0.611}$  (16).  $D_{\text{eff}}$  therefore exceeds  $D_{\text{bulk}}$  for molecules larger than  $L \approx 490 \text{ nm}$ , a value corresponding to only a few DNA Kuhn segments. The surprising dispersion properties of DNA in small channels beg the development of a microscopic model. Flexible polymers differ crucially from point-like or rigid particles in that they possess many internal degrees of freedom. These may enable DNA to explore the parabolic flow more effectively, leading to an enhanced apparent diffusivity. These are also at the root of entropic elasticity (35), which would tend to confine the molecular center of mass to the center of the channel, thereby suppressing Taylor dispersion relative to that of point particles, while permitting fluctuations absent in rigid-particle models.

The high effective diffusion coefficient that can account for the reduced hydrodynamic dispersion of DNA in small channels is not caused by a high center of mass self-diffusion. Indeed,  $D_0$  is a measure of molecular self-diffusion and was found to decrease with decreasing  $h$  (Fig. 4). At low  $R_g/h$ , the ratio  $D_0/D_{\text{bulk}}$  was nearly 1, and it decayed slowly with  $R_g/h$  for  $R_g/h \geq 0.1$ . Above  $R_g/h \approx 0.5$ , the self-diffusion of DNA decreased rapidly as  $D_0/D_{\text{bulk}} \propto (R_g/h)^{-2/3}$ . This scaling relationship was predicted by Brochard and de Gennes (36) for sufficiently small channels in which highly confined molecules expand laterally, leading to a higher viscous drag and hence a reduced self-diffusion coefficient. First confirmed experimentally in a narrow tube geometry (37), this behavior has been modeled by computer simulations and experimentally verified for  $R_g/h$  as high as 1 in a slit geometry (26, 38). Here we see that  $D_0/D_{\text{bulk}} \propto (R_g/h)^{-2/3}$  to  $R_g/h$  values as high as 7.<sup>1</sup>

<sup>1</sup>An additional  $h = 107 \text{ nm}$  channel was used to test the scaling of  $D_0$  to high degrees of confinement.

In conclusion, we have shown how the pressure-driven transport behavior of DNA molecules in microfluidic and nanofluidic channels is dominated by the statistical properties of polymer coils. The distribution of a random-flight polymer across a channel leads to a pressure-driven mobility that increases with molecular length in large channels and remains independent of length in channels that are small compared with molecular coil size. The Taylor dispersion of DNA molecules is highly suppressed in confined channels and decays with channel height and molecular length according to a power-law scaling relationship. These polymer transport properties are of considerable significance to bioanalysis technology aimed at the separation of DNA by length or the uniform transport of DNA molecules through a fluidic system. An understanding of DNA transport characteristics can therefore guide the design of fluidic channels, the fundamental components of lab-on-a-chip technology.

## Materials and Methods

Microfluidic and nanofluidic channels were prepared by using a sodium silicate bonding procedure (39). The 50- $\mu\text{m}$ -wide and 4-mm-long channels were connected to large access holes at either end. The channel height,  $h$ , ranged from 175 nm to 3.8  $\mu\text{m}$ . The channels were filled with buffer solution by capillarity and then electrophoretically cleaned of ionic impurities by applying 50 V across the channel for  $\approx 10 \text{ min}$ . A DNA solution was introduced into the channels via the access holes, which were then connected to open fluid reservoirs (10-ml glass syringe bodies) via Peek tubing, all filled with bubble-free buffer solution. The fluorescently labeled DNA molecules were imaged with an electron multiplication CCD camera (Andor, Belfast, Ireland) at a rate of 5 Hz by using an inverted oil-immersion fluorescence microscope ( $\times 100$ , 1.4 N.A.; Olympus, Tokyo, Japan) focused at the channel midplane.

The trajectories of DNA molecules were determined by using custom-developed molecular tracking software (Matlab; Mathworks, Natick, MA) that locates a molecule's center of mass as the first moment of the intensity distribution and follows it over a series of images. The integrated fluorescence intensity and the second moment of the intensity distribution (an estimate of  $R_g$ ) were also calculated for each molecule and used as criteria to filter imaging noise, damaged DNA fragments, or overlapping molecules. Molecular trajectories were verified by eye to ensure faithful tracking. Ambiguous molecular trajectories that would intersect, divide (break), or irreversibly stick to the channel were manually excluded.

The three linear DNA fragments studied were as follows: 48,502-bp, unmethylated  $\lambda$ -phage DNA ( $\lambda$ -DNA; Promega, Leiden, The Netherlands); a 20,262-bp pBluescript 2 $\times$  Topo plasmid construct (Stratagene, La Jolla, CA); and an 8,778-bp pBluescript+ 1,2,4  $\lambda$ -DNA fragment plasmid construct (Stratagene). The DNA fragments were fluorescently labeled with YOYO-1 dye (Molecular Probes, Eugene, OR) using a base pair to dye ratio of 6:1 and suspended in an aqueous solution containing 50 mM NaCl, 10 mM Tris, 1 mM EDTA (pH 8.0), and 2% 2-mercaptoethanol by volume to minimize photobleaching. The concentration of DNA molecules was adjusted to introduce a convenient density ( $\approx 1$ –20 in an 80- $\mu\text{m}$ -wide field of view) into each fluidic device tested.

We thank Peter Veenhuizen and Susanne Hage for preparing DNA fragments; Jerry Westerweel and Rene Delfos for assistance in calibrating fluid viscosities; Serge Lemay, Theo Odijk, and Cees Storm for useful discussions; and Andor Technology for the use of a camera. This work was supported by the Netherlands Organization for Scientific Research, Fundamenteel Onderzoek der Materie, and NanoNed.

1. Volkmoth WD, Austin RH (1992) *Nature* 358:600–602.
2. Han J, Craighead HG (2000) *Science* 288:1026–1029.
3. Li J, Stein D, McMullan C, Branton D, Aziz MJ, Golovchenko JA (2001) *Nature* 412:166–169.

4. Storm AJ, Chen JH, Ling XS, Zandbergen HW, Dekker C (2003) *Nat Mater* 2:537–540.
5. Perkins TT, Smith DE, Chu S (1997) *Science* 276:2016–2021.
6. Smith DE, Chu S (1998) *Science* 281:1335–1340.

7. Smith DE, Babcock HP, Chu S (1999) *Science* 283:1724–1727.
8. Schroeder CM, Babcock HP, Shaqfeh ESG, Chu S (2003) *Science* 301:1515–1519.
9. Quake SR, Babcock H, Chu S (1997) *Nature* 388:151–154.
10. Tegenfeldt JO, Prinz C, Cao H, Chou S, Reisner WW, Riehn R, Wang, Y M, Cox EC, Sturm JC, Silberzan P, Austin RH (2004) *Proc Natl Acad Sci USA* 101:10979–10983.
11. Stone HA, Stroock AD, Ajdari A (2004) *Annu Rev Fluid Mech* 36:381–411.
12. Squires TM, Quake SR (2005) *Rev Mod Phys* 77:977–1026.
13. Dimarzio EA, Guttman CM (1970) *Macromolecules* 3:131–146.
14. Brenner H, Gaydos LJ (1977) *J Colloid Interface Sci* 58:312–356.
15. Taylor G (1953) *Proc R Soc London Ser A* 219:186–203.
16. Smith DE, Perkins TT, Chu S (1996) *Macromolecules* 29:1372–1373.
17. Darnton N, Bakajin O, Huang R, North B, Tegenfeldt JO, Cox EC, Sturm J, Austin RH (2001) *J Phys Condens Matter* 13:4891–4902.
18. Weast RC, ed (1982) *CRC Handbook of Chemistry and Physics* (CRC, Boca Raton, FL), 63rd Ed.
19. Casassa EF, Tagami Y (1969) *Macromolecules* 2:14–26.
20. Casassa EF (1967) *J Polym Sci B Polym Lett* 5:773–778.
21. Fleer GJ, Skvortsov AM, Tuinier R (2003) *Macromolecules* 36:7857–7872.
22. Tjissen R, Bleumer JPA, van Krevelde ME (1983) *J Chromatogr* 260:297–304.
23. Tjissen R, Bos J, van Krevelde ME (1986) *Anal Chem* 58:3036–3044.
24. Doi M, Edwards SF (1986) *The Theory of Polymer Dynamics* (Oxford Univ Press, Oxford).
25. Babcock HP, Smith DE, Hur JS, Shaqfeh ESG, Chu S (2000) *Phys Rev Lett* 85:2018–2021.
26. Jendrejack RM, Dimalanta ET, Schwartz DC, Graham MD, de Pablo JJ (2003) *Phys Rev Lett* 91:038102.
27. Jendrejack RM, Schwartz DC, de Pablo JJ, Graham MD (2004) *J Chem Phys* 120:2513–2529, and correction (2004) 120:6315.
28. Segre G, Silberberg A (1961) *Nature* 189:209–210.
29. Ma HB, Graham MD (2005) *Phys Fluids* 17:083103.
30. Fang L, Hu H, Larson RG (2005) *J Rheol* 49:127–138.
31. Brenner H (1980) *PhysicoChem Hydrodyn* 1:91–123.
32. Dutta D, Leighton DT (2003) *Anal Chem* 75:57–70.
33. Frankel I, Mancini F, Brenner H (1991) *J Chem Phys* 95:8636–8646.
34. Brenner H, Nadim A, Haber S (1987) *J Fluid Mech* 183:511–542.
35. Bustamante C, Marko JF, Siggia ED, Smith S (1994) *Science* 265:1599–1600.
36. Brochard F, de Gennes PG (1977) *J Chem Phys* 67:52–56.
37. Cannell DS, Rondelez F (1980) *Macromolecules* 13:1599–1602.
38. Chen YL, Graham MD, de Pablo JJ, Randall GC, Gupta M, Doyle PS (2004) *Phys Rev E Stat Phys Plasmas Fluids Relat Interdiscip Top* 70:060901.
39. Stein D, Kruithof M, Dekker C (2004) *Phys Rev Lett* 93:035901.
40. Blom MT, Chmela E, Oosterbroek RE, Tjissen R, van den Berg A (2003) *Anal Chem* 75:6761–6768.